Available online at www.sciencedirect.com
ScienceDirect
European Journal of Pharmaceutics and Biopharmaceutics 70 (2008) 66–74
European Journal of Pharmaceutics and Biopharmaceutics
www.elsevier.com/locate/ejpb

Research paper

# Three-step tumor targeting of paclitaxel using biotinylated PLA-PEG nanoparticles and avidin–biotin technology: Formulation development and in vitro anticancer activity

Mika Pulkkinen [a,*], Jere Pikkarainen [b], Thomas Wirth [b], Tommy Tarvainen [a], Vesa Haapa-aho [c], Harri Korhonen [c], Jukka Seppälä [c], Kristiina Järvinen [a]

[a] Department of Pharmaceutics, University of Kuopio, Kuopio, Finland
[b] Department of Molecular Medicine and Biotechnology, University of Kuopio, Kuopio, Finland
[c] Department of Chemical Technology, Helsinki University of Technology, Helsinki, Finland

Received 9 January 2008; accepted in revised form 21 April 2008
Available online 29 April 2008

**Abstract**

Despite recent advances in cancer therapy, many malignant tumors still lack effective treatment and the prognosis is very poor. Paclitaxel is a potential anticancer drug, but its use is limited by the facts that paclitaxel is a P-gp substrate and its aqueous solubility is poor. In this study, three-step tumor targeting of paclitaxel using biotinylated PLA-PEG nanoparticles and avidin–biotin technology was evaluated in vitro as a way of enhancing delivery of paclitaxel. Paclitaxel was incorporated both in biotinylated (BP) and non-biotinylated (LP) PEG-PLA nanoparticles by the interfacial deposition method. Small (mean size ~ 110 nm), spherical and slightly negatively charged (−10 mV) BP and LP nanoparticles achieving over 90% paclitaxel incorporation were obtained. The successful biotinylation of nanoparticles was confirmed in a novel streptavidin assay. BP nanoparticles were targeted in vitro to brain tumor (glioma) cells (BT4C) by three-step avidin–biotin technology using transferrin as the targeting ligand. The three-step targeting procedure increased the anti-tumoral activity of paclitaxel when compared to the commercial paclitaxel formulation Taxol® and non-targeted BP and LP nanoparticles. These results indicate that the efficacy of paclitaxel against tumor cells can be increased by this three-step targeting method.


*Keywords:* Paclitaxel; Nanoparticle; Biotin–avidin technology; Anti-tumoral activity; Glioma

## 1. Introduction

There are many cases where the administration of anticancer drugs is limited by their unsatisfactory properties such as poor solubility, narrow therapeutic window and P-glycoprotein (P-gp) substrate specificity. For example, paclitaxel is a very promising chemotherapy agent but unfortunately it shows poor aqueous solubility. The currently available commercial formulation Taxol® contains Cremophor EL (polyethoxylated castor oil) and ethanol as excipients to promote solubilization. Cremophor EL can induce severe side-effects including hypersensitivity reactions, nephrotoxicity and neurotoxicity [1]. In addition to the formulation problems, paclitaxel is a substrate for the P-gp transporter which impedes the permeability of the drug through physiological barriers and prevents it from gaining access to tumor tissue [2–5].

Paclitaxel targeting utilizing stealth nanoparticles made of hydrophobic polymers could solve some of the problems associated with paclitaxel delivery. No harmful excipients are needed to formulate paclitaxel preparations if nanoparticles prepared from hydrophobic polymers are used for the drug delivery. When compared to non-stealth nanoparti-

* Corresponding author. Department of Pharmaceutics, University of Kuopio, P.O. Box 1627, FIN-70211 Kuopio, Finland. Tel.: +358 17 163556; fax: +358 17 163549.
*E-mail address:* Mika.Pulkkinen@uku.fi (M. Pulkkinen).

0939-6411/$ - see front matter © 2008 Elsevier B.V. All rights reserved.
doi:10.1016/j.ejpb.2008.04.018

cles, stealth nanoparticles show extended blood circulation times, resulting in a better tissue distribution [6]. Tumor targeting of drug may be achieved either by a direct targeting method or by resorting to the pretargeting multistep method. In the case of direct targeting, the targeting ligand is attached onto the nanoparticles. Whereas in the case of the pretargeting method, the ligand, intended to be concentrated and localized in the tumor, is administered before the administration of drug-loaded carrier. Typically the pretargeting method results in a longer circulation time of the nanoparticles after repeated dosing when compared to directly targeted nanoparticles [7]. This can be explained by the fact that the pretargeting method does not unfavorably change the physicochemical properties of the nanoparticles since it is not necessary to attach a targeting ligand, such as a large antibody, onto the surface of the nanoparticles.

The use of avidin–biotin technology may represent a versatile approach to target nanoparticles into the tumor tissue. The avidin–biotin bond is the strongest protein–ligand interaction known in nature [8]. The avidin–biotin technology has long been utilized in immunohistochemistry and molecular biology [9]. Recently, this technology has been applied for drug targeting [10–14]. The three-step method using avidin–biotin technology that is used in human imaging and therapy of cancer tissue [15–18] includes the following steps: (i) i.v. administration of biotinylated targeting ligands, (ii) i.v. administration of avidin and (iii) i.v. administration of biotinylated drug or drug-loaded carrier.

The aim of this study was to develop paclitaxel-loaded stealth nanoparticles which could be targeted into the cancer cells via three-step avidin–biotin technology. To achieve this goal, PLA-PEG-biotin polymer was synthesized and characterized. Biotinylated paclitaxel-loaded nanoparticles were prepared by the interfacial deposition method. The resulting formulations were characterized in terms of size, charge, morphology, drug encapsulation and drug release. Furthermore, the functionality of biotinylated nanoparticles was assessed by a newly developed biotin–avidin affinity assay. The in vitro cytotoxicity of the nanoparticles was evaluated against glioma cells (BT4C) using biotinylated transferrin as a targeting ligand.

## 2. Materials and methods

### 2.1. Materials

Paclitaxel (from Taxus yannanensis) (T-1912) was obtained from Sigma–Aldrich Co. Ltd. (St. Louis, USA). Taxol® was supplied by Bristol-Myers Squibb (New York, USA). D,L-Lactide was purchased from Purac (Gorinchem, Netherlands). Me-PEG-OH (~2000 g/mol) was obtained from Fluka (Seelze, Germany). HO-PEG-$NH_2$ was purchased from Nektar Therapeutics ($M_w = 3400$ g/mol, Huntsville, AL, USA). NHS-biotin, triethylamine, stannous octoate, Dulbecco's modified Eagle's medium and Eagle's minimum essential medium were products of Sigma–Aldrich Co. Ltd. (St. Louis, USA). L-Glutamine, non-essential amino acids and sodium pyruvate were provided by Gibco (Grand Island, NY, USA). Biotinylated transferrin (A-2666), neutravidin and 1% glutamax were products of Molecular Probes (Leiden, Netherlands) while fetal bovine serum was from HyClone (Logan, Utah, USA). CellTiter-Blue™ reagent was obtained from Promega (Southampton, UK). Sterile water and NaCl 0.9% were obtained from Baxter (Vantaa, Finland) and deionized water was processed by a Milli-Q system (Millipore). Other reagents were of reagent grade.

### 2.2. Polymer synthesis and characterization

#### 2.2.1. PLA-PEG-biotin synthesis by solution polymerization

Polymer synthesis was performed using the method of Salem et al. with slight modifications [19]. Briefly, biotin-PEG-OH was prepared as follows. 1 g of HO-PEG-$NH_2$ ($M_w$: 3400 g/mol) was dissolved in 2 ml of acetonitrile at room temperature. Triethylamine (80 μl) and dichloromethane (1 ml) were added and mixture was stirred for 1 min. Next, NHS-biotin (0.25 g) was added and stirring was continued overnight under argon. The mixture was filtered and the biotin-PEG-OH polymer was precipitated with an excess of diethyl ether. The precipitated polymer was filtered and purified by dissolving it into hot 2-propanol (70 °C) and then allowed to cool down. The reprecipitated polymer was then filtered again. Water residues were removed by dissolving the polymer in toluene and refluxing for 4 h with a Dean-Stark trap. The toluene was evaporated and the polymer was dried in a vacuum.

Purified biotin-PEG-OH (0.3 g) and D,L-lactide (1.8 g) were dissolved in 10 ml of toluene and the mixture heated to 70 °C. Stannous octoate solution in toluene (0.03 mol% in relation to D,L-lactide) was added and the reaction was carried out by refluxing at 111 °C for 4.5 h under argon. After reaction, toluene was removed with vacuum distillation and the reaction was completed under argon flow for 1 h at 140 °C. The product was purified by precipitating the polymer from dichloromethane solution (10 ml) by adding it to an excess of cool diethyl ether. The PLA-PEG-biotin polymer was dried and stored in a vacuum. The reaction steps were followed by $^1H$ NMR analysis which confirmed that the products contained the desired structures.

#### 2.2.2. PLA-PEG synthesis by melt polymerization

PLA-PEG was prepared by melt polymerization using stannous octoate (0.03 mol%) as an initiator and Me-PEG-OH as a co-initiator. A round-bottomed flask was charged with D,L-lactide (25.9 g) and Me-PEG-OH (2.5 g). Polymerization was carried out at 140 °C with magnetic stirring under argon for 16 h. After polymerization, the product was purified by precipitating the polymer/dichloromethane solution with an excess of hexane, and dried in a vacuum.

### 2.3. Polymer characterization

Molecular weights ($M_w$, $M_n$) were determined by size exclusion chromatography (SEC) (Waters System Interface module, Waters 510 HPLC Pump, Waters 410 Differential Refractometer, Waters 717plus autosampler, and four linear PL gel columns: $10^4$, $10^5$, $10^3$ and 100 Å connected in series) The flow rate of the chloroform was 1 ml/min and the injection volume was 200 μl. Before analysis, the samples were filtered through a 0.5-μm Millex SR filter. Monodisperse polystyrene standards were used for the calibration.

More accurate structures of the prepared polymers were provided by $^1$H NMR. For $^1$H NMR measurements, the samples were dissolved in DMSO-$d_6$ in 5-mm NMR tubes at room temperature. The sample concentration was about 1.0% by weight. NMR spectra were recorded on a Varian Gemini 2000 spectrometer working at 300 MHz for protons.

Melting temperatures ($T_m$) and glass transition temperatures ($T_g$) were measured by differential scanning calorimetry (DSC) (Mettler Toledo Star) in a nitrogen environment. Samples (5–10 mg) were heated twice, at a rate of 10 °C/min, to ensure that their thermal histories were similar. The temperature range was between −100 and 250 °C. The melting temperature and glass transition temperature were determined from the second heating scan.

### 2.4. Preparation of nanoparticles

Nanoparticles were prepared by the interfacial deposition solvent displacement method [20]. Briefly, 1 mg of PLA-PEG-biotin and 99 mg of PLA-PEG (BP) or 100 mg of PLA-PEG (LP) were dissolved in 1 ml of acetone containing 1 mg of paclitaxel. The mixture was vortexed until solids dissolved and then 9 ml of acetone was added into the solution just before adding the organic phase drop-wise into 10 ml of water phase (4 ml NaCl 0.9% and 6 ml $H_2O$) with magnetic stirring. The suspension was allowed to stabilize with stirring for 5 min. Acetone and the surplus of water were removed by rotavapor (BÜCHI, Flawil, Switzerland) at 25 °C under nitrogen flow. The suspension was kept at 200 mbar for 2 h to remove all of the acetone from the solution. The suspension was made up to a volume of 4 ml with water and sonicated for 2 min (Finnsonic m03, Lahti, Finland) to brake cluster of particles. Finally, suspension was filtered through 1.2 μm membrane filter to remove aggregates and non-incorporated drug. Unloaded nanoparticles were prepared using the same procedure without the drug. For cell studies, all steps were completed aseptically with sterilized equipment.

### 2.5. Physicochemical characterization of nanoparticles

#### 2.5.1. Determination of drug amount

The amount of paclitaxel in nanoparticles was determined using the previously described extraction method with slight modifications [21]. The paclitaxel content was determined both from the nanoparticle suspension and from washed lyophilized nanoparticles. In the case of the suspension method, 100 μl of aqueous nanoparticle suspension was dried under a nitrogen stream and the drug content in the dried nanoparticles was determined as described below. The washed lyophilized nanoparticles were prepared as follows: 0.5 ml of nanoparticle aqueous suspension was centrifuged (Heraeus Biofuge 17 RS, Heraeus Sepatech, Hanau, Germany) at 17,000 rpm for 30 min (+20 °C). Then the sample was washed with 1 ml of Mq-water and centrifuged again. The resulting pellet was frozen (−86 °C) and dried with freeze dryer for 24 h (FST Systems Inc., New York, USA). Either the exactly weighed nitrogen stream-dried nanoparticles (~2.5 mg) or the lyophilized nanoparticles (~2.5 mg) were dissolved in 1 ml of DCM and then 5 ml of acetonitrile–water (50:50) solution was added and the mixture was vortexed vigorously for 2 min. A nitrogen stream was introduced until the polymer precipitated and a clear solution was obtained. The solutions with precipitated polymer were centrifuged for 10 min at 5000 rpm (Megafuge 1.0R, Heraeus instruments, Hanau, Germany) and the supernatant was collected. This was followed by wash with 5 ml of acetonitrile–water (50:50) and centrifugation at 5000 rpm for 10 min. The supernatant was collected and the samples were made up to volume with acetonitrile–water (50:50), and the paclitaxel concentration was analyzed by HPLC as described below. The extraction efficiency of paclitaxel was determined as follows: equal concentrations of paclitaxel and polymer when compared to their concentration in the nanoparticles were dissolved in 1 ml of DCM and extraction was performed as described above. The extraction efficiency of paclitaxel was 95.6% ($n = 5$, SD = 2.6) and this value was used to calculate the amount of drug in the particles.

The Gilson HPLC system consisted of a detector (UV/VIS-151), pump (321), autoinjector (234), interface (Hercule Lite for Borwin 1.5) and integrator (Borwin 1.5). The mobile phase consisted of a mixture of acetonitrile and water (50:50 v/v). A reverse-phase Supelcosil® C-18 column (150 × 4.6 mm id, pore size 5 μm, Supelco, Bellefonte, USA) was used for the chromatographic separation with an injection volume of 20 μl. Paclitaxel was detected at 227 nm and the area under the curve was used for quantification. The calibration curve of the paclitaxel was linear over the range 0.05–50 μg/ml with a correlation coefficient of $R^2 \geqslant 0.999$).

The encapsulation efficiencies of the drug loading were calculated using Eqs. (1) and (2), respectively.

$$\text{Encapsulation efficiency (\%)} = (\text{paclitaxel amount in nanoparticles(mg)}/\text{initial drug amount(mg)}) \times 100\% \quad (1)$$

$$\text{Drug loading (\%)} = (\text{paclitaxel amount in nanoparticles(mg)}/\text{dry weight of nanoparticles(mg)}) \times 100\% \quad (2)$$

*2.5.2. In vitro drug release*

The in vitro release of paclitaxel from nanoparticles was determined by the ultracentrifugation method. A total of 40 μl of nanoparticle aqueous suspension was added into 5 ml of pH 7.4 phosphate-buffered saline solution containing 0.2% of sodiumlaurylsulfate (SLS). SLS was added into the release medium to enhance the solubility of paclitaxel. The nanoparticle sample contained about 10 μg of paclitaxel in the release studies. The solubility of paclitaxel in the release medium was analyzed to be 38 μg/ml, and thus the release studies were conducted under sink conditions (maximum paclitaxel concentration in release medium was 2 μg/ml). Nanoparticles were incubated in 10 ml tubes at a frequency of 120 strokes/min at 37 °C (Grant OLS200, Cambridge, UK). Samples were withdrawn at predetermined time points and nanoparticles were separated by high-speed centrifugation at 25,000 rpm for 30 min at 4 °C in a Beckman Avanti J-30I centrifuge (rotor JA-25.15, 74200 G). The concentration of paclitaxel in the supernatant was determined by the HPLC as described in Section 2.5.1.

*2.5.3. Particle size distribution, morphology and zeta-potential of nanoparticles*

Particle mean size and size distribution were measured by the light scattering method using Nicomp Zeta Potential/Particle Sizer (model 380 XLS, NicompTM, Santa Barbara, CA). The nanoparticle suspension was diluted in purified water before the measurement. The zeta-potential of the nanoparticles was measured by the Malvern Zetasizer 3000HS (Malvern Instruments, UK), and the suspension samples were diluted in 20 mM Hepes (pH 7.4). For each sample, the mean value of at least 10 measurements was calculated.

The morphology of the nanoparticles was studied by transmission electron microscopy (TEM) (JEM-1200EX, JEOL Ltd., Tokyo, Japan). A drop of nanoparticle suspension diluted in water was placed on a carbon-coated copper grid. After 1 min, the sample was washed with ultra-purified water and the excess of fluid was removed by a piece of filter paper. Finally, the sample was negative stained with 2% phosphotungstic acid solution for 30 s. and the excess of the fluid removed and the dry sample analyzed.

*2.5.4. Biotin-affinity assay*

The accessibility and functionality of biotin on the surface of nanoparticles were evaluated by the biotin–streptavidin binding method. Nanoparticles with (BP) and without (LP) biotin were diluted in filtered (0.45 μm) binding buffer (20 mM sodium phosphate, 0.15 M NaCl, pH 7.5). A HiTrap™ streptavidin HP column (Amersham Biosciences, Uppsala, Sweden) was equilibrated with the binding buffer according to product instructions. The samples were pumped into the column by peristaltic pump at a flow rate of 0.1 ml/min. The fraction of outcoming (i.e. not bound) nanoparticles was measured by two techniques: an HPLC-GPC method and a light scattering method (NICOMP). The light scattering method was based on the intensity value which is proportional to the amount of particles. HPLC system, described in Section 2.5.1, was used with a size exclusion column (PL aquagel-OH Mixed 8 μm, 300 × 7.5 mm, Polymer Labs, UK) and 100 μl injection volume. The HPLC measurement was performed at 225 nm with a flow rate of 0.4 ml/min using binding buffer as a mobile phase. Standard curves were made by diluting the nanoparticle suspension in binding buffer.

*2.6. In vitro anti-tumoral activity*

BT4C cells, rat glioma cell line, were cultured in Dulbecco's modified Eagle's medium supplemented with 10% fetal bovine serum and 1% glutamax. HepG2 cells, Human hepatocellular liver carcinoma cell line, were grown in Eagle's minimum essential medium adjusted to contain 1.5 g/L sodium bicarbonate and supplemented with 2 mM L-glutamine, 0.1 mM non-essential amino acids, 1.0 mM sodium pyruvate, 10% FBS, penicillin (100 IU/ml) and streptomycin (100 μg/ml). Cells were grown in an atmosphere of 95% humidified air and 5% $CO_2$ at 37 °C. Exponential growth was maintained using appropriate splitting and renewal of medium. For the experiments, cells were seeded onto 96-well plates (Cellstar) at a density of 10,000 cells/well and incubated overnight.

The effects of studied formulations at paclitaxel concentrations from 0.1 to 50 μg/ml on cell viability were studied in the presence and absence of targeting. The three-step method was used for the targeting of paclitaxel-loaded biotinylated nanoparticles (BP), i.e. (1) cells were incubated with biotinylated transferrin (50 μg/ml) for 15 min, (2) cells were incubated with neutravidin (50 μg/ml) for 5 min and (3) cells were incubated with BP nanoparticles for 15 min. The one-step method was used for the non-targeted paclitaxel-loaded biotinylated (BP) and non-biotinylated (LP) nanoparticles and for Taxol®, i.e. cells were incubated with BP or LP nanoparticles or Taxol for 15 min. After every step, the wells were washed with 200 μl of PBS (pH 7.4). Then, cells were incubated with culture medium (200 μl/well) for 3 days. In every case, the BP, LP and Taxol® samples were diluted in culture medium and administered to the cells in a volume of 100 μl/well.

After 3 days' growth, 100 μl of fresh culture medium was changed to the cells and cell viability was assessed by adding 20 μl of CellTiter-blue reagent. The assay is based on the reductive ability of living cells to metabolize resazurin into a fluorescent end-product resorufin. After 2 h of incubation, the measurements were conducted fluorometrically by a Victor multiplate system (excitation 544 nm and emission 590 nm, Perkin–Elmer, HTS 7000 Plus, Bio Assay Reader/Victor$^2$ 1420 multilabel counter, Perkin Elmer, Turku, Finland). Cell viability was calculated by Eq. (3):

$$\text{Cell viability } (\%) = (\text{Fluorescence}_{\text{test cells}}/\text{Fluorescence}_{\text{control cells}}) \times 100 \quad (3)$$

where $Fluorescence_{control\ cells}$ is the fluorescence of control cells incubated with cell culture media only.

### 2.7. Statistical analysis

A non-parametric Kruskal–Wallis test was used to test the statistical significance of differences between groups. Significance in the differences of the means was tested using the Mann–Whitney test. The level of significance was taken as $P < 0.05$.

## 3. Results

### 3.1. Polymerization

The biotinylated and pegylated polylactides were successfully polymerized using solution polymerization and melt polymerization, respectively. More specific details of the polymers are given in Table 1. The attachment of biotin was confirmed by $^1$H NMR (Fig. 1) and DSC measurements. Two urea protons from the cyclic biotin can be seen in the biotin-NHS (data not shown), biotin-PEG-OH and PLA-PEG-biotin spectra at 6.33 and 6.40 ppm. Due to the low concentration of biotin, the signal is very low in PLA-PEG-biotin spectrum. The covalent bond between biotin-NHS and HO-PEG-$NH_2$ was confirmed from the free amido proton signal at 7.81 ppm (NHCO). Melting temperatures for biotin-NHS and HO-PEG-$NH_2$ were 216 and 61 °C, respectively. Furthermore, DSC revealed only one peak for biotin-PEG-OH at 54 °C also confirming that no free biotin was present.

### 3.2. Characterization of nanoparticles

Nanoparticles were successfully prepared by the interfacial deposition solvent displacement method using as the polymer either PLA-PEG (LP) or mixtures of PLA-PEG and PLA-PEG-biotin (BP). Paclitaxel was encapsulated effectively both within the LP and BP nanoparticles as >90% incorporation was obtained in both cases (Table 2). The encapsulation efficiency of washed lyophilized nanoparticles was close to that achieved with direct measurement from the nanoparticle suspension. This confirmed that the drug had been effectively incorporated into the nanoparticles. The size of both LP and BP nanoparticles was close to 100 nm with a fairly narrow-size distribution (Table 2). As an example, the TEM picture reveals the spherical shape and homogeneous size distribution of the BP nanoparticles (Fig. 2). Both LP and BP nanoparticles exhibited negative surface charge with zeta-potential values close to −10 mV. It can be concluded that biotinylation of nanoparticles did not substantially change the characteristics of the nanoparticles when compared to LP nanoparticles.

### 3.3. Biotin-affinity assay

The presence of functional biotin on the surface of the nanoparticles was confirmed by the developed biotin-affinity assay, i.e. nanoparticles were pumped through the streptavidin column and the fraction of unbound nanoparticles was determined. Biotin molecules bind to avidin and therefore biotinylated nanoparticles (BP) are retained inside the column whereas nanoparticles without functional biotin (LP) are not retained. Both HPLC-GPC and light scattering (NICOMP) methods confirmed that the biotinylated nanoparticles had been effectively bound into the streptavidin column whereas non-biotinylated nanoparticles were not bound (Fig. 3).

### 3.4. In vitro release study

The in vitro release of paclitaxel from biotinylated nanoparticles is shown in Fig. 4. The release profile shows a high burst release during the first hour followed by a slower drug release. Virtually all of the paclitaxel was released within 24 h. The biotinylation of nanoparticles did not change the release profile of paclitaxel since the profiles were identical for BP (Fig. 4) and LP nanoparticles (data not shown in Fig. 4 for the sake of clarity).

### 3.5. In vitro anti-tumoral activity

The effects of Taxol®, paclitaxel-loaded LP nanoparticles and paclitaxel-loaded non-targeted and targeted BP nanoparticles were studied on glioma (BT4C) and hepatic (HepG2) cell viability. Paclitaxel was evaluated in the concentration range of 0.1–50 μg/ml (equivalent to BP and LP nanoparticle concentrations up to 5 mg/ml). In the case of each formulation, cell viability decreased with an increase in the paclitaxel concentration (Fig. 5). Incubation of cells with unloaded LP or BP nanoparticles or neutravidin or biotinylated transferrin did not evoke any cytotoxicity since the cell viability value remained >90% (data not shown).

When compared to Taxol®, paclitaxel-loaded non-targeted LP or BP nanoparticles were not more effective against brain tumor cells at the tested concentrations (Fig. 5). When the effects of the formulations on control

Table 1
Molecular weights ($M_w$, $M_n$), glass transition temperatures ($T_g$), melting temperatures ($T_m$) and polydispersities ($M_w/M_n$) of studied polymers

| Polymer | PEG-chain (g/mol) | $M_w$ (g/mol) | $M_n$ (g/mol) | $M_w/M_n$ | $T_g$ (°C) | $T_m$ (°C) |
|---|---|---|---|---|---|---|
| PLA-PEG | 2000 | 40,500 | 20,000 | 2.0 | 35 | – |
| PLA-PEG-biotin | 3400 | 22,600 | 19,900 | 1.1 | 15 | – |

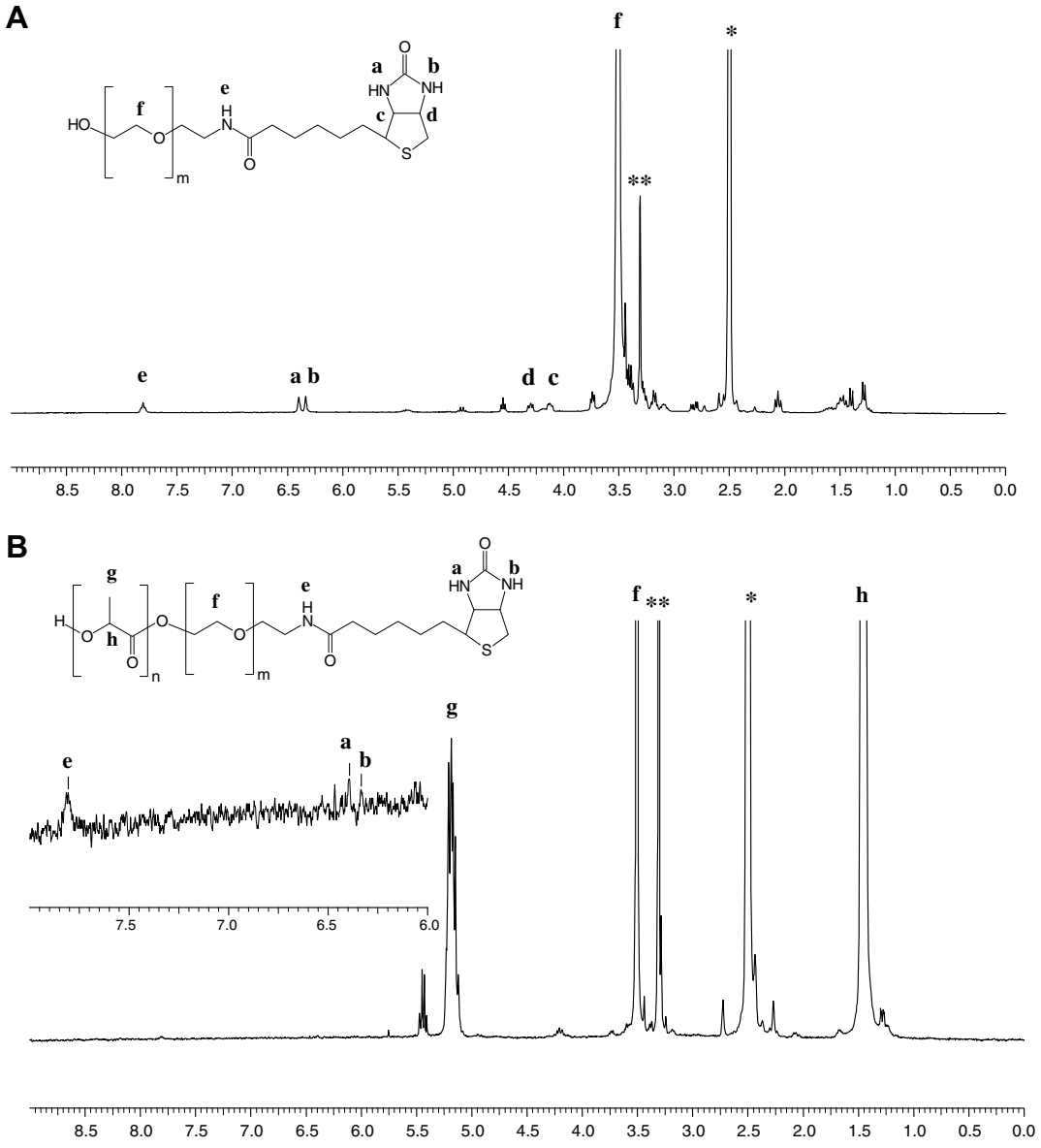


Fig. 1. $^{1}$H NMR spectra of synthesized PEG-biotin-OH (A) and PLA-PEG-biotin (B) in DMSO-$d_6$. Characteristic peaks of biotin are shown in the close-up detail for PLA-PEG-biotin. *DMSO peak, **$H_2O$ peak.

Table 2
Size, encapsulation efficiency and zeta-potential of paclitaxel-loaded (1% w/w) non-biotinylated (LP) and biotinylated (BP) nanoparticles

| Nanoparticles | Size (nm) | Encapsulation efficiency (%) (washed) | Encapsulation efficiency (%) (suspension) | Zeta-potential (mV) |
|---|---|---|---|---|
| LP | $104.9 \pm 38.6^{*}$ | $92.9 \pm 3.1$ | $93.5 \pm 5.2$ | $-10.4 \pm 0.5$ |
| BP | $106.8 \pm 38.5$ | $93.7 \pm 5.0$ | $92.4 \pm 3.9$ | $-10.2 \pm 0.5$ |

Encapsulation efficiency was determined by two methods as described in Section 2.5.1. Data are presented as means ± SD ($n = 3$–4, except: $^{*}n = 5$, SD of the nanoparticles is shown as the mean of SD value of the Nicomp apparatus).

cell viability (HepG2) were studied, the three-step targeting procedure did not increase the anti-tumoral activity of paclitaxel when compared to non-targeted BP nanoparticles (data not shown). Instead, the three-step targeting procedure using BP nanoparticles increased significantly the cytotoxicity of paclitaxel at concentrations of 10 and 50 μg/ml when compared to Taxol® and non-targeted BP and LP nanoparticles. However, the potency of this targeted formulation decreased when more diluted samples were used.

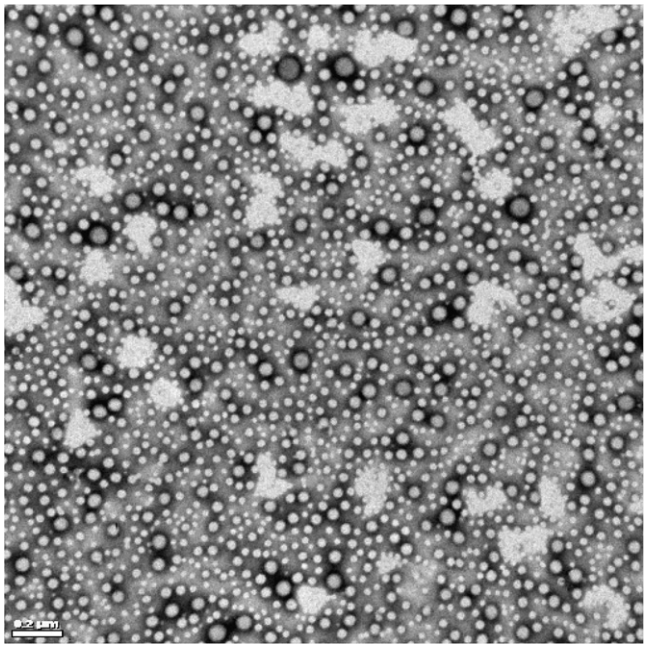

Fig. 2. TEM photograph of biotinylated nanoparticles (BP). Scale bar 200 nm (magnification 50,000×).

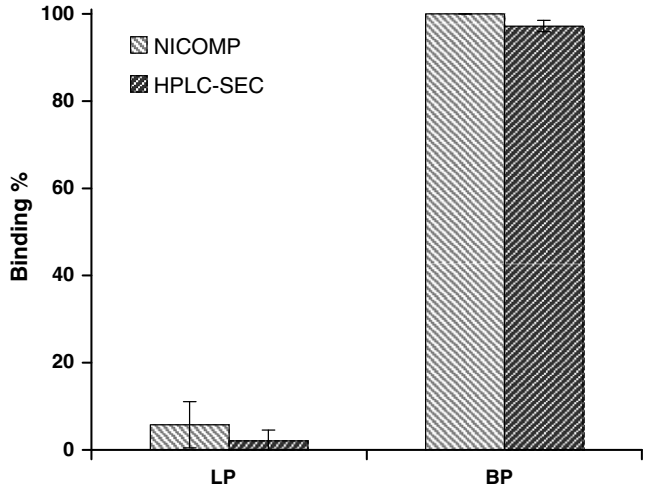


Fig. 3. Binding of biotinylated (BP) and non-biotinylated (LP) nanoparticles in the streptavidin column ($n = 3$, ± SD are shown). Measurements were made by NICOMP light scattering and HPLC-SEC methods.

## 4. Discussion

Paclitaxel is a potent anticancer drug and its use is restricted by its poor aqueous solubility and by the fact that paclitaxel is a P-gp substrate. The poor aqueous solubility requires the inclusion of a harmful excipient, Cremophor EL, in Taxol®. The commercial non-targeted paclitaxel nanoparticulate formulation Abraxane®, based on albumin, does not contain Cremophor EL. It can be postulated that targeted nanoparticles made of hydrophobic materials could further enhance the potency of paclitaxel therapy.

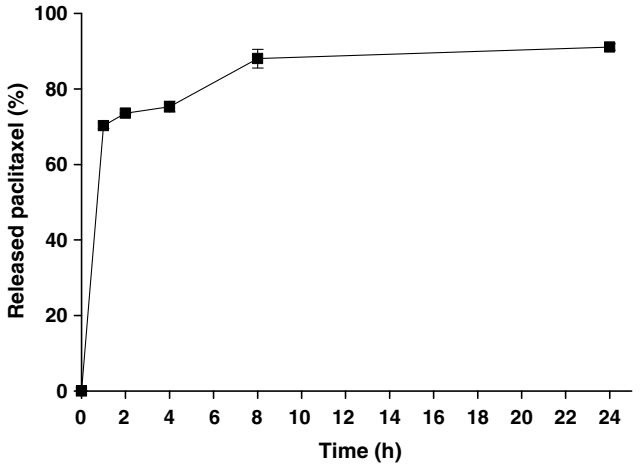


Fig. 4. In vitro release rate of paclitaxel from biotinylated nanoparticles (BP) in PBS (pH 7.4) with 0.2% SLS at 37 °C (mean ± SD, $n = 4$).

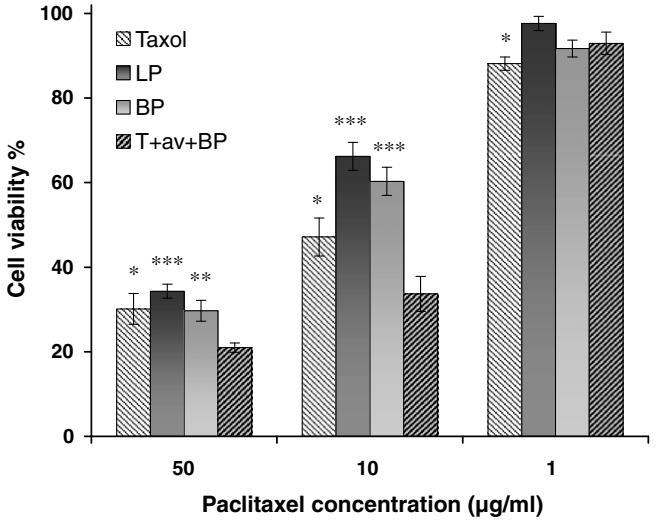


Fig. 5. Viability of glioma cells (BT4C) after incubation with Taxol®, nanoparticles (LP), biotinylated nanoparticles (BP) and biotinylated nanoparticles with the three-step targeting using biotinylated transferrin (T) and neutravidin (av). Data are presented as means ± SEM ($n = 15$–16). $^{*}$, $^{**}$ and $^{***}$ statistically different from the value of targeted nanoparticles (T + av + BP) ($^{*}P < 0.05$, $^{**}P < 0.01$, $^{***}P < 0.001$ by Kruskal–Wallis, Mann–Whitney's U-test).

In the present study, a rapid and reproducible preparation method was developed which resulted in the production of spherical paclitaxel-loaded biotinylated and non-biotinylated nanoparticles with a narrow particle size distribution (size about 100 nm) and a slightly negative surface charge. The negative surface charge of the particles may be attributable to the carboxylic groups of polylactic acid. The present zeta-potential value of LP nanoparticles (−10 mV) is in agreement with earlier studies where zeta-potential values for pegylated or polyvinyl alcohol-covered PLA-based nanoparticles have been reported [22–24]. Interestingly, biotinylation did not markedly change the surface charge of nanoparticles, though biotin is known to possess a positive charge. The paclitaxel release from

the nanoparticles was rapid and virtually all of drug was released within 24 h (Fig. 4). The fast release of the drug is probably caused by the large surface area of the nanoparticles and the short diffusional distance. It has also been reported earlier that paclitaxel release from PLA-based nanoparticles is rapid in vitro [25]. It can be concluded that the present nanoparticles should be well suited for i.v. dosing in terms of physicochemical properties since it is known that long-lasting circulating injected nanoparticles should be small, slightly negatively charged and covered with a protective PEG layer [6].

Avidin has four binding sites for biotin molecules, and the binding sites are close to each other which leads to steric hindrance [9]. In the case of biotinylated stealth nanoparticles, also the dense PEG layer on nanoparticle surface can cause steric hindrance, resulting in a decrease in the activity of biotin. Therefore, the biotinylated conjugates should be separated by spacers in order to achieve optimal biotin–avidin binding. In the present study, the biotin-PEG-PLA possessed a longer PEG chain (3400 g/mol) than PEG-PLA (2000 g/mol). It was confirmed that BP nanoparticles resulted in binding of biotin to avidin (Fig. 3).

A glioma cell line (BT4C) was used to evaluate the antitumoral activity of paclitaxel-loaded nanoparticles and Taxol®. Brain tumors are a serious form of cancer as the prognosis of patients with primary tumors or brain metastases is very poor since there are few effective treatments against this aggressive disease [26–28]. For example, the prognosis of the fairly common malignant primary brain tumors such as glioma, is very unsatisfactory with less than one-year medium survival [29]. Usually, brain tumors are treated by brain irradiation or surgery [30,31]. The use of chemotherapy is less common because of the poor abilities of most chemotherapy agents to cross the blood brain barrier (BBB) due to tight endothelium and P-gp activity. Targeted nanoparticles may enhance paclitaxel delivery to the brain tumor after i.v. administration because nanoparticles are known to be able to penetrate through the BBB [32–35]. The BBB is probably more leaky in the region of the tumor than in normal brain due to enhanced vasculature which will increase the permeation of nanoparticles to these sites [31,36]. Furthermore, paclitaxel has a radiosensitizing ability against glioma which makes it an interesting candidate for treatment of brain tumors since these malignancies are usually treated by radiotherapy [37].

In the present study, transferrin was selected as a targeting ligand because transferrin receptors are highly expressed on tumor cells and the brain capillary endothelium [38,39]. Transferrin is an iron-transporting serum glycoprotein which is efficiently taken up into cells by receptor-mediated endocytosis. Previously, transferrin has been successfully used to target various molecules and liposomes into tumor and brain tissue [39–43]. The present result indicates that the three-step targeting procedure increases markedly anti-tumoral activity of paclitaxel when compared to the commercial paclitaxel formulation Taxol® and non-targeted biotinylated (BP) and non-biotinylated nanoparticles (LP) (at paclitaxel concentrations of 10 and 50 μg/ml). Moreover, without the targeting steps, drug-loaded LP and BP nanoparticles did not show substantially different cytotoxicities against BT4C cells. An earlier study also indicated that biotinylation of nanoparticles did not enhance the cellular uptake of the non-targeted nanoparticles [44].

## 5. Conclusions

Paclitaxel-loaded biotinylated PLA-PEG nanoparticles were successfully prepared. The produced nanoparticles displayed a high drug-encapsulation efficiency and active functional biotin on their surface. The three-step targeting procedure using biotinylated nanoparticles increased markedly anti-tumoral activity of paclitaxel at concentrations of 10 and 50 μg/ml when compared to Taxol® or the non-targeted nanoparticles. These results suggest that the efficacy of paclitaxel against tumor cells may be increased by the three-step targeting method.

## Acknowledgments

The financial support from the Academy of Finland (Grant #104544), Emil Aaltonen Foundation as well as the Association of Finnish Pharmacies is gratefully acknowledged. Also, Samuli Hirsjärvi is acknowledged for guidance in the zeta-sizer experiments.

## References

[1] A.K. Singla, A. Garg, D. Aggarwal, Paclitaxel and its formulations, Int. J. Pharm. 235 (2002) 179–192.
[2] E.K. Rowinsky, P.J. Burke, J.E. Karp, R.W. Tucker, D.S. Ettinger, R.C. Donehower, Phase I and pharmacodynamic study of Taxol in refractory acute leukemias, Cancer Res. 49 (1989) 4640–4647.
[3] S. Fellner, B. Bauer, D.S. Miller, M. Schaffrik, M. Fankhanel, T. Spruh, G. Bernhardt, C. Graeff, L. Farber, H. Gschaidmeier, A. Buschsuer, G. Fricker, Transport of paclitaxel (Taxol) across the blood–brain barrier in vitro and in vivo, J. Clin. Invest. 10 (2002) 1309–1317.
[4] J.J. Heimans, J.B. Vermorken, J.G. Wolbers, C.M. Eeltink, O.W.M. Meijer, M.J.B. Taphoorn, J.H. Beijnen, Paclitaxel (Taxol) concentrations in brain tumor tissue, Ann. Oncol. 5 (1994) 951–953.
[5] A. Sparreboom, J. van Asperen, U. Mayer, A.H. Schinkel, J.W. Smit, D.K. Meijer, P. Borst, W.J. Nooijen, J.H. Beijnen, O. van Tellingen, Limited oral bioavailability and active epithelial excretion of paclitaxel (Taxol) caused by P-glycoprotein in the intestine, Proc. Natl. Acad. Sci. USA 94 (1997) 2031–2035.
[6] J.-C. Olivier, Drug transport to brain with targeted nanoparticles, NeuroRx® 2 (2005) 108–119.
[7] J.A. Harding, C.M. Engbers, M.S. Newman, N.I. Goldstein, S. Zalipsky, Immunogenicity and pharmacokinetic attributes of poly(ethylene glycol)-grafted immunoliposomes, Biochim. Biophys. Acta 1327 (1997) 181–192.
[8] N.M. Green, Avidin, Adv. Protein Chem. 29 (1975) 85–105.
[9] D.A. Goodwin, C.F. Meares, Advances in pretargeting biotechnology, Biotech. Adv. 19 (2001) 435–450.
[10] K. Hoya, L.R. Guterman, L. Miskolczi, L.N. Hopkins, A novel intravascular drug delivery method using endothelial biotinylation and avidin–biotin binding, Drug Deliv. 8 (2001) 215–222.

[11] E.K. De La Fuente, C.A. Dawson, L.D. Nelin, R.D. Bongard, T.L. McAuliffe, M.P. Merker, Biotinylation of membrane proteins accessible via the pulmonary circulation in normal and hyperoxic rats, Am. J. Physiol. 272 (1997) L461–L470.
[12] O.C. Boerman, F.G. Van Schaijk, W.J. Oyen, F.H. Corstens, Pretargeted radioimmunotherapy of cancer: progress step by step, J. Nucl. Med. 44 (2003) 400–411.
[13] L. Nobs, F. Buchegger, R. Gurny, E. Allémann, Biodegradable nanoparticles for direct or two-step tumor immunotargeting, Bioconjug. Chem. 17 (2006) 139–145.
[14] J.A. Rodríguez, G. Helguera, T.R. Daniels, I.I. Neacato, H.E. López-Valdés, A.C. Charles, M.L. Penichet, Binding specificity and internalization properties of an antibody–avidin fusion protein targeting the human transferrin receptor, J. Control. Release 124 (2007) 35–42.
[15] G. Paganelli, R. Orecchia, B. Jereczek-Fossa, C. Grana, M. Cremonesi, F. De Braud, N. Tradati, M. Chinol, Combined treatment of advanced oropharyngeal cancer with external radiotherapy and three-step radioimmunotherapy, Eur. J. Nucl. Med. 25 (1998) 1336–1339.
[16] M. Cremonesi, M. Ferrari, M. Chinol, M.G. Stabin, C. Grana, G. Prisco, C. Robertson, G. Tosi, G. Paganelli, Three-step radioimmunotherapy with yttrium-90 biotin: dosimetry and pharmacokinetics in cancer patients, Eur. J. Nucl. Med. 26 (1999) 110–112.
[17] H.B. Breitz, D.R. Fisher, M.L. Goris, S. Knox, B. Ratliff, A.D. Murtha, P.L. Weiden, Radiation absorbed dose estimation for 90Y-DOTA-biotin with pretargeted NR-LU-10/streptavidin, Cancer Biother. Radiopharm. 14 (1999) 381–395.
[18] S.J. Knox, M.L. Goris, M. Tempero, P.L. Weiden, L. Gentner, H. Breitz, G.P. Adams, D. Axworthy, S. Gaffican, K. Bryan, D.R. Fisher, D. Colcher, I.D. Horak, L.M. Weiner, Phase II trial of yttrium-90-DOTA-biotin pretargeted by NR-LU-10 antibody/streptavidin in patients with metastatic colon cancer, Clin. Cancer Res. 6 (2000) 406–414.
[19] A.K. Salem, S.M. Cannizzaro, M.C. Davies, S.J.B. Tendler, C.J. Roberts, P.M. Williams, K.M. Shakesheff, Synthesis and characterization of a degradable poly(lactic acid)–poly(ethylene glycol) copolymer with biotinylated end groups, Biomacromolecules 2 (2001) 575–580.
[20] H. Fessi, F. Puisieux, J.P. Devissaguet, N. Ammoury, S. Benita, Nanocapsule formation by interfacial polymer deposition following solvent displacement, Int. J. Pharm. 55 (1989) R1–R4.
[21] Y.M. Wang, H. Sato, I. Adachi, I. Hirikoshi, Preparation and characterization of poly(lactic-co-glycolic acid) microspheres for targeted delivery of a novel anticancer agent, Taxol, Chem. Pharm. Bull. 44 (1996) 1935–1940.
[22] Y. Mo, L.Y. Lim, Preparation and in vitro anticancer activity of wheat germ agglutinin (WGA)-conjugated PLGA nanoparticles loaded with paclitaxel and isopropyl myristate, J. Control. Release 107 (2005) 30–42.
[23] Y. Dong, S.-S. Feng, Methoxy poly(ethylene glycol)-poly(lactide) (MPEG-PLA) nanoparticles for controlled delivery of anticancer drugs, Biomaterials 25 (2004) 2843–2849.
[24] T. Riley, T. Covender, S. Stolnik, C.D. Xiong, M.C. Garnett, L. Illum, S.S. Davis, Colloidal stability and drug incorporation aspects of micellar-like PLA-PEG nanoparticles, Colloids Surf. B Biointerfaces 16 (1999) 147–159.
[25] C. Fonseca, S. Simões, R. Gaspar, Paclitaxel-loaded PLGA nanoparticles: preparation, physicochemical characterization and in vitro anti-tumoral activity, J. Control. Release 83 (2002) 273–286.
[26] P.L. Kornblith, M. Walker, Chemotherapy for malignant gliomas, J. Neurosurg. 68 (1988) 1–17.
[27] L.M. De Angelis, Brain tumors, N. Engl. J. Med. 344 (2001) 114–123.
[28] Z.R. Cohen, D. Suki, J.S. Weinberg, E. Marmor, F.F. Lang, D.M. Gershenson, R. Sawaya, Brain metastases in patients with ovarian carcinoma: prognostic factors and outcome, J. Neurooncol. 66 (2004) 313–325.
[29] C.B. Scott, C. Scarantino, R. Urtasun, B. Movsas, C.U. Jones, J.R. Simpson, A.J. Fischbach, W.J. Curran, Validation and predictive power of radiation therapy oncology group (RTOG) recursive partitioning analysis classes for malignant glioma patients: a report using RTOG 90-06, Int. J. Radiat. Oncol. Biol. Phys. 40 (1998) 51–55.
[30] S. Sathornsumetee, D.A. Reardon, A. Desjardins, J.A. Quinn, J.J. Vredenburgh, J.N. Rich, Molecularly targeted therapy for malignant glioma, Cancer 110 (2007) 13–24.
[31] M.J. van den Bent, The role of chemotherapy in brain metastases, Eur. J. Cancer 39 (2003) 2114–2120.
[32] S.C. Steiniger, J. Kreuter, A.S. Khalansky, I.N. Skidan, A.I. Bobruskin, Z.S. Smirnova, S.E. Severin, R. Uhl, M. Kock, K.D. Geiger, S.E. Gelperina, Chemotherapy of glioblastoma in rats using doxorubicin-loaded nanoparticles, Int. J. Cancer 109 (2004) 759–767.
[33] J.M. Koziara, P.R. Lockman, D.D. Allen, R.J. Mumper, Paclitaxel nanoparticles for the potential treatment of brain tumors, J. Control. Release 99 (2004) 259–269.
[34] A.E. Gulyaev, S.E. Gelperina, I.N. Skidan, A.S. Antropov, G.Y. Kivman, J. Kreuter, Significant transport of doxorubicin into the brain with polysorbate 80-coated nanoparticles, Pharm. Res. 16 (1999) 1564–1569.
[35] P.R. Lockman, M.O. Oyewumi, J.M. Koziara, K.E. Roder, R.J. Mumper, D.D. Allen, Brain uptake of thiamine-coated nanoparticles, J. Control. Release 93 (2003) 271–282.
[36] D.J. Steward, A critique of the role of the blood–brain barrier in the chemotherapy of human brain tumors, J. Neurooncol. 20 (1994) 121–139.
[37] R.B. Tishler, C.R. Geard, E.J. Hall, P.B. Schiff, Taxol sensitizes human astrocytoma cells to radiation, Cancer Res. 52 (1992) 3495–3497.
[38] E. Wagner, D. Curiel, M. Cotton, Delivery of drugs, proteins and genes into cells using transferrin as a ligand for receptor mediated endocytosis, Adv. Drug Deliv. Rev. 14 (1994) 113–135.
[39] J. Huwyler, D. Wu, W.M. Pardridge, Brain drug delivery of small molecules using immunoliposomes, Proc. Natl. Acad. Sci. USA 93 (1996) 14164–14169.
[40] N. Shi, Y. Zhang, C. Zhu, R.J. Boado, W.M. Pardridge, Brain-specific expression of an exogenous gene after i.v. administration, Proc. Natl. Acad. Sci. USA 98 (2001) 12754–12759.
[41] K. Maruyamaa, O. Ishidaa, S. Kasaokaa, T. Takizawaa, N. Utoguchia, A. Shinoharab, M. Chibab, H. Kobayashic, M. Eriguchid, H. Yanagie, Intracellular targeting of sodium mercaptoundecahydrododecaborate (BSH) to solid tumors by transferrin-PEG liposomes, for boron neutron-capture therapy (BNCT), J. Control. Release 98 (2004) 195–207.
[42] A. Gijsens, A. Derycke, L. Missiaen, D. de Vos, J. Huwyler, A. Eberle, P. de Witte, Targeting of the photocytotoxic compound AlPcS4 to Hela cells by transferrin conjugated PEG-liposomes, Int. J. Cancer 101 (2002) 78–85.
[43] O. Ishida, K. Maruyama, H. Tanahashi, M. Iwatsuru, K. Sasaki, M. Eriguchi, H. Yanagie, Liposomes bearing polyethyleneglycol-coupled transferrin with intracellular targeting property to the solid tumors in vivo, Pharm. Res. 18 (2001) 1042–1048.
[44] R. Gref, P. Couvreur, G. Barratt, E. Mysiakine, Surface-engineered nanoparticles for multiple ligand coupling, Biomaterials 24 (2003) 4529–4537.